

Two phase transitions in the two-dimensional nematic 3-vector model with no quasi long-range order: Monte Carlo simulation of the density of states

B. Kamala Latha¹ and V.S.S. Sastry²

¹*School of Physics, University of Hyderabad, Hyderabad 500046, India and*

²*Centre for Modelling, Simulation and Design, University of Hyderabad, Hyderabad 500046, India*

(Dated: June 20, 2018)

The presence of stable topological defects in a two-dimensional ($d = 2$) liquid crystal model allowing molecular reorientations in three dimensions ($n = 3$) was largely believed to induce defect-mediated Berzenskii-Kosterlitz-Thouless (BKT) type transition to a low temperature phase with quasi long-range order. However, earlier Monte Carlo (MC) simulations could not establish certain essential signatures of the transition, suggesting further investigations. We study this model by computing its equilibrium properties through MC simulations, based on the determination of the density of states of the system. Our results show that, on cooling, the high temperature disordered phase deviates from its initial progression towards the topological transition, crossing over to a new fixed point, condensing into a nematic phase with exponential correlations of its director fluctuations. The thermally induced topological kinetic processes continue, however limited to the length scales set by the nematic director fluctuations, and lead to a second topological transition at a lower temperature. We argue that in the ($d = 2, n = 3$) system with a biquadratic Hamiltonian, the presence of additional molecular degree of freedom and local Z_2 symmetry associated with lattice sites, together promote the onset of an additional relevant scaling field at matching length scales in the high temperature region, leading to a crossover.

PACS numbers: 64.70.M-, 64.70.mf

Two-dimensional ($d = 2$) liquid crystal (LC) models with molecular reorientations in three dimensions ($n = 3$) host stable topological point defects (disclination points) with half integral charge [1] owing to their apolar order parameter (OP) geometry (real two-dimensional projective space RP^2), and are predicted to undergo a topological phase transition [2]. Several Monte Carlo (MC) studies on Lebwohl-Lasher (LL) model [3] confined to a two-dimensional square lattice were carried out based on the Metropolis algorithm, alluding to a Berzenskii-Kosterlitz-Thouless type [4] topological transition to a low-temperature phase with quasi long-range order (QLRO) [2, 5–9]. This assignment could not be conclusive however, primarily because of the absence of size-invariant Binder’s cumulant [10] at the reported transition temperature [11, 12]. Recent comparative analysis of the MC data based on finite size scaling criterion [13] distinguishes the RP^2 -systems from other two-dimensional magnetic systems, *viz.* 2d-XY and 2d-Heisenberg models, and concludes that the 2d LC systems could only have pseudo-critical regions. A plausible conjecture advanced to account for the observed inconsistency has been the presence of an underlying subtle and persistent crossover in the model [9, 11, 12].

In this context, we examined this model with a different MC sampling procedure: we derived the equilibrium properties of this model by first computing its density of states (DoS) and then constructing equilibrium ensembles. The DoS was obtained with a variant of the MC procedure, - entropic sampling technique [14] -, which is geared to access the configuration space uniformly with respect to energy. We used a modified version of the

Wang-Landau algorithm [15] augmented with *frontier-sampling* [16] technique to enhance its efficacy [17]. We constructed entropic ensembles comprising of microstates distributed uniformly with energy by performing a random walk biased by the DoS of the system. We distinguish the equilibrium ensembles obtained by reweighting procedure from the entropic ensemble (say, *RW*-ensembles) from those obtained based on the Metropolis algorithm, (*B*-ensembles) [17], while comparing their equilibrium averages of different physical properties.

We considered a square ($d = 2$) lattice of variable size $L \times L$ ($L = 50, 80, 100, 120, 150$), each lattice site hosting a manifold of directions in three dimensional space ($n = 3$). The interactions are described by the Lebwohl-Lasher Hamiltonian, $H = -\epsilon \sum_{\langle i,j \rangle} P_2(\cos \theta_{ij})$, with the summation covering all the nearest neighbours, and prescribing periodic boundary conditions. P_2 is the second Legendre polynomial and θ_{ij} is the angle between the neighbouring molecules. The temperature (T) is reported in reduced units scaled by the coupling strength ϵ . The *RW*-ensembles are constructed from the entropic ensemble [17], in the temperature range of interest ($T = 0.4$ to 1.0 , with a resolution of 0.001). We computed, as a function of T , the averages of energy E , nematic order parameter S , nematic susceptibility χ , as well as Binder’s cumulant R_4 associated with S to monitor the transition ([17]). In addition, we also calculated the average values of the density of unbound defects D_t as well as topological order parameter δ based on algorithms described in [2, 8]. Orientational pair correlation function $G(r_{ij}) = \langle P_2(\cos \theta_{ij}) \rangle$ was computed (at $L = 150$) at about 40 temperatures covering the above range. The

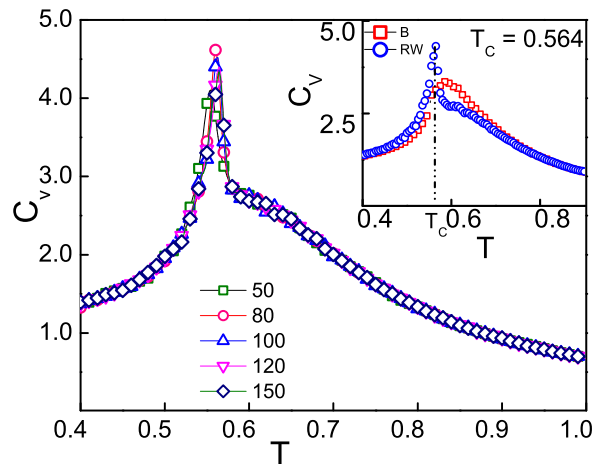


FIG. 1: (color online) Temperature variation of specific heat (per site) from RW -ensembles at sizes $L = 50, 80, 100, 120, 150$. Inset shows qualitatively different temperature variations of C_v from RW - and B -ensembles at $L = 150$.

averages of E , S , D_t and δ have statistical errors (estimated using Jack-knife algorithm [18]) typically of the order of 1 in 10^4 , while the higher moments (C_v , χ , R_4) are relatively less accurate, estimated to be about 5 in 10^3 .

We now present qualitatively differing features of the physical parameters obtained from the two types of sampling procedures, leading to a discussion on the interpretation of our observations. Fig. 1 shows an essentially size-independent temperature variation of C_v (per site) as obtained from RW -ensembles at different system sizes, indicating an initial development of a broad cusp on cooling, but yielding to an abrupt sharp peak located at 0.564 ($L=150$). This is to be contrasted with the broad cusp obtained from the B -ensemble at the same size (shown in the Inset of Fig. 1), which is in accord with the data reported earlier. Fig. 2 depicts the temperature dependence of χ from RW -ensembles as a function of size. Its temperature variations as obtained from the two ensembles are compared in the Inset (a) at $L = 150$. The corresponding order parameters are shown in Inset (b). The values of the order parameter S in the low temperature phase were found to decrease with size as computed from B -ensembles (consistent with the QLRO regime), while RW -ensembles essentially report its size-independence for $L \geq 80$ (not shown here). Low temperature values of the susceptibility also qualitatively differ (Inset (a)): it is non-zero and diverging with size in the B -ensembles, while its value quickly tends to zero with the present sampling procedure. Also, the χ peaks in the present study shift slightly towards higher temperature with size, very similar to C_v .

The absence, from the earlier Monte Carlo studies, of a size-invariant Binder's cumulant (R_4) at the predicted transition temperature has been a major obstacle to un-

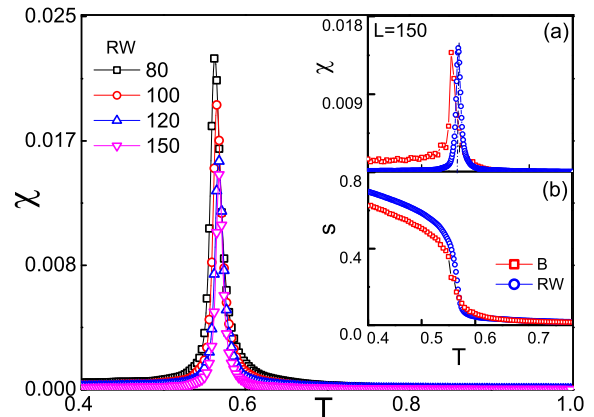


FIG. 2: (color online) Temperature variation of nematic susceptibility χ from RW -ensembles at sizes $L = 80, 100, 120$ and 150 . Insets (a) and (b) depict the comparison of the temperature variations of χ and nematic order S from RW -ensembles with B -ensembles at $L = 150$.

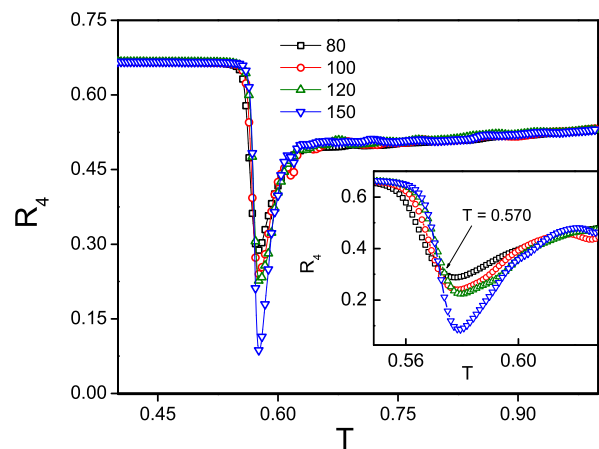


FIG. 3: (color online) Temperature variation of Binder's cumulant of the nematic order R_4 from RW -ensembles at sizes $L = 80, 100, 120$ and 150 . Inset shows the magnified version near the transition.

ambiguously assign the transition as defect-mediated, required to explain the observed low temperature QLRO phase [11, 12]. From our data based on the DoS, a size-independent cumulant value was obtained at $T = 0.570 \pm 0.001$ (Fig. 3 and Inset), providing a confirmatory evidence of a (continuous) transition at this temperature, as also representing the thermodynamic limit of the size-dependent C_v peak positions Fig. 1. We investigate the nature of the low temperature phase by computing the spatial dependences of the orientational correlations of LC molecules at $L = 150$. Variations of $G(r)$ with distance (in lattice units), at different temperatures spanning the window $T = 0.4$ to 0.9 , are shown in Fig. 4. Qualitatively differing from the earlier observations of

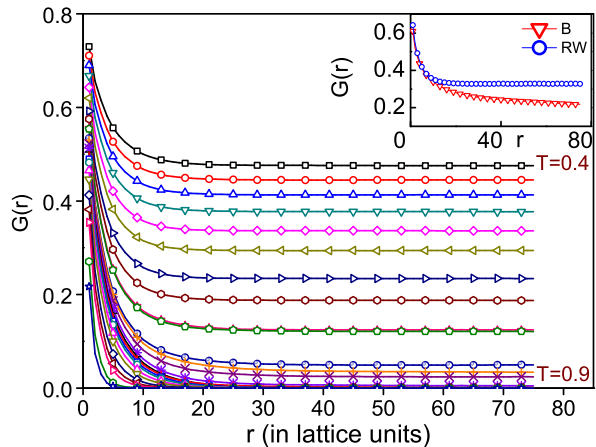


FIG. 4: (color online) Variation of the orientational pair correlation function $G(r)$ with lattice distances ($L = 150$) in the temperature range $T = 0.4$ to 0.9 . The inset compares the $G(r)$ obtained from B - and RW -ensembles in the low temperature phase, at $T = 0.5$.

power law variation at low temperatures, $G(r)$ fit very well to exponential decays, leading to the determination of the correlation length $\xi(T)$ (to within about 1% error). The Inset compares $G(r)$ obtained from RW - and B -ensembles at $T = 0.5$ (low-temperature phase), at $L = 150$. The B -ensemble data require a power law for a satisfactory fit, as concluded by the earlier studies. Presence of a single length scale in the system at any temperature is the major indicator signalling a qualitative departure from the current interpretation of the low temperature phase in terms of QLRO.

We show the temperature variation of $\xi(T)$ in Fig. 5. Starting from the high temperature side, $\xi(T)$ initially tends to diverge, but deviates away near $T \approx 0.6$ to form a cusp at 0.564 . We analyse the high temperature data ($\xi(T)$ vs T in Fig. 5) assigning its divergence as due to the temperature dependent kinetics of the unbound defects, given by $\xi(T) \sim \exp[\frac{A}{(T-T_U)^{1/2}}]$ in the mean-field limit [4]. Here T_U is the limiting temperature for the unbound defects to exist and A is a constant. The present data fit to this expression very satisfactorily till about $T \simeq 0.6$ (Fig.5), yielding an estimate of the unbinding transition temperature $T_{U_\xi} = 0.471 \pm 0.005$. This implies that, but for the interruption by the transition at T_c , the system would have proceeded to a direct topological transition with a broad C_v cusp terminating its critical contribution in the neighbourhood of T_{U_ξ} as a weak essential singularity. The departure of the observed ξ from its expected divergence (shown as dotted lines in Fig. 5) forming a cusp at $T = 0.564$, as well as concomitant de-

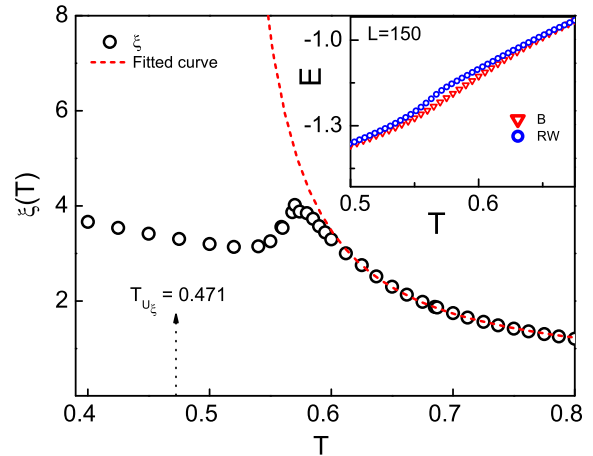


FIG. 5: (color online) Variation of correlation length ξ as a function of temperature. The dotted line represents the extrapolated divergence of ξ based on high temperature data (see text). Inset shows the variation of energy with temperature near the peak position from both the ensembles.

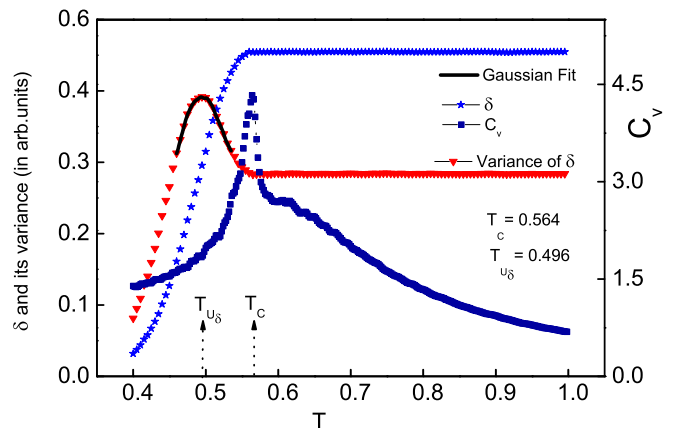


FIG. 6: (color online) Temperature variation of topological order δ (stars) and of its variance (triangles) superposed on the specific heat C_v profile (squares). Solid line indicates a local Gaussian fit to the cusp of the variance.

velopment of a sharp C_v peak at the same temperature show a crossover of the system towards a new fixed point from its initial progression towards a topological transition. The inset of this figure shows the differences in the energies (per site) as computed by the two MC procedures in the crossover region. The Metropolis algorithm accesses lower energy microstates in locating the regions of equilibrium ensembles, while the density of states computation samples relatively higher energy microstates, - both being guided however by the same requirement of free energy minimization.

The temperature variation of δ associated with the topological order [2], along with C_v is depicted in Fig. 6.

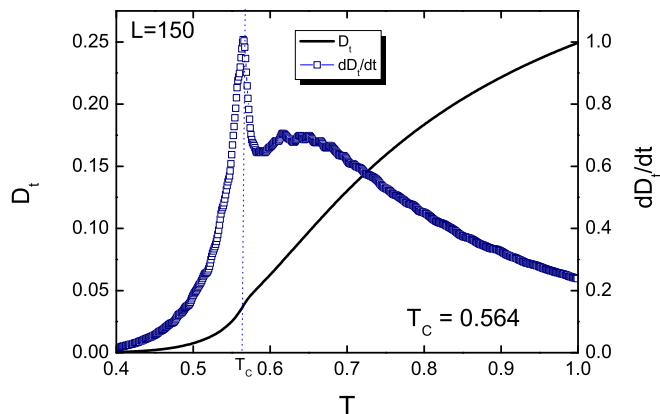


FIG. 7: (color online) Temperature variation of defect density D_t from RW -ensembles at $L = 150$, superposed by its temperature derivative.

The variance of δ (in arbitrary units for plotting convenience) is also shown in the same figure. The location of the peak of this variance is determined by fitting a local Gaussian, leading to an estimate of the unbinding transition temperature at $T_{U_\delta} \simeq 0.496$. This value is close to $T_{U_\xi} \simeq 0.471$, estimated from the high temperature divergence of $\xi(T)$. Distinct values of T_{U_δ} and T_c point clearly to the presence of two transitions in this system. In Fig. 7 we show the temperature variation of D_t along with its temperature derivative at $L = 150$. D_t shows a rather sharp change in its slope at the location of the C_v peak, (which is absent in the B -ensemble data), and the profile of its temperature derivative is qualitatively very similar to that of C_v (Fig. 1). The source of energy contribution to the observed C_v peak is closely connected with the rate of the defect density production, - a clear manifestation of the qualitative changes in the relevant length scale in this temperature region.

The crossover of the system as it is cooled initially from a high temperature disordered phase is connected with the development of an additional relevant scaling field in the parameter space, as the increasing correlation length (arising from the diminishing number density of the unbound defects) matches typical nearest neighbour distances in lattice units. The apolar nature of the local directors associated with the lattice sites (Z_2 symmetry) in the presence of an attractive biquadratic Hamiltonian, and facilitated by the extra degree of molecular reorientation ($n = 3$), lead to the development of critical nematic clusters at these coherence lengths. The transition at T_c is thus from the isotropic to a nematic phase, with the $\xi(T)$ on either side of the transition at T_c being limited by different mechanisms, - critical fluctuations on the high temperature side and nematic director fluctuations at low temperatures -, thus forbidding the

development of QLRO regime. The system crosses over towards this fixed point for $T \leq 0.6$. The phase immediately below the T_c with a single temperature-dependent length scale represents an interesting nematic medium which has unbound topological defects undergoing thermally activated kinetic processes, but their length scales being limited by the coherence lengths of the director fluctuations. Similar scenario was noticed earlier in fully frustrated anti-ferromagnetic Heisenberg (HAFT) model on a triangular lattice which also hosts RP^2 topology for its order parameter space [19]. In this ($d = 2$ and $n = 3$) magnetic model, spin fluctuations were found to limit the diverging correlation length in the high temperature paramagnetic phase. The second transition in the LC system estimated by δ at T_{U_δ} ($\simeq 0.496$), is mediated by the topological defects, leading to a lower temperature nematic phase with growing average cluster size and hosting only bound topological defects. In HAFT models, such media were referred to as spin gel phases.

We conclude that the presence of the extra dimension for molecular freedom, coupled with the local gauge invariance under Z_2 symmetry are ideally suited to induce a crossover when the development of the orientational correlation length to a sufficient degree makes the attractive interaction of the LL model a relevant scaling field. The failure of the earlier MC studies to associate a size-invariant Binder's cumulant at the proposed topological transition temperature seems to be justifiably conjectured as due to an underlying crossover, but the conventional MC sampling method could not access the higher energy microstates apparently needed in this temperature region (Inset of Fig. 5) to locate the true minimum free energy configurations, thus missing to detect the crossover phenomenon.

We acknowledge the computational support from the Centre for Modelling Simulation and Design (CMSD) and the School of Computer and Information Sciences (DST PURSE - II Grant) at the University of Hyderabad. BKL acknowledges financial support from Department of Science and Technology, Government of India vide grant ref No: SR/WOS-A/PM-2/2016 (WSS) to carry out this work.

-
- [1] N. D. Mermin, Rev. Mod. Phys. **51**, 591 (1979).
 - [2] H. Kunz and G. Zumbach, Phys. Rev. B **46**, 662 (1992).
 - [3] P. A. Lebowitz and G. Lasher, Phys. Rev. A **6**, 426 (1973).
 - [4] V. L. Berezenskii, Sov. Phys. JETP **32**, 493 (1971); V. L. Berezenskii, Sov. Phys. JETP **34**, 610 (1972); J. M. Kosterlitz, and D. J. Thouless, J. Phys. C **6**, 1181 (1973).
 - [5] C. Chiccoli, P. Pasini and C. Zannoni, Physica **148A** 298 (1988).
 - [6] B. Berche and R. Paredes, Condensed Matter Physics, **8**, 723 (2005).
 - [7] E. Mondal and S. K. Roy, Physics Letters A **312**, 397

- (2003).
- [8] S. Dutta and S. K. Roy, Phys. Rev. E **70**, 066125 (2004).
- [9] S. Shabnam, S. D. Gupta and S. K. Roy, Physics Letters A **380**, 667 (2016).
- [10] K. Binder, Z. Phys. B Cond. Matter. **43**, 119 (1981).
- [11] R. Paredes V, A. I. Farinas-Sanchez and R. Botet, Phys. Rev. E **78**, 051706 (2008).
- [12] A. I. Farinas-Sanchez, R. Botet, B. Berche and R. Parades, Cond. Matter. Physics **13**, 13601 (2010).
- [13] Y. Tomita, Phys. Rev. E **90**, 032109 (2014).
- [14] F. Wang and D. P. Landau, Phys. Rev. Lett. **86**, 2050 (2001); F. Wang and D. P. Landau, Phys. Rev. E **64**, 056101 (2001).
- [15] D. Jayasri, V. S. S. Sastry, and K. P. N. Murthy, Phys. Rev. E **72**, 036702 (2005).
- [16] C. Zhou, T. C. Schulthess, S. Torbrugge and D. P. Landau, Phys. Rev. Lett. **96**, 120201 (2006).
- [17] B. Kamala Latha, R. Jose, K. P. N. Murthy and V. S. S. Sastry, Phys. Rev. E **92**, 012505 (2015).
- [18] B. Kamala Latha, G. Sai Preeti, K. P. N. Murthy and V. S. S. Sastry, Comp. Mat. Sci. **118**, 224 (2016).
- [19] H. Kawamura, A. Yamamoto and T. Okubo, J. Phys. Soc. Japan **79**, 023701 (2010).